Diffraction separation based on perturbed CRS attributes

Jorge H. Faccipieri Jr., Leiv J. Gelius and Martin Tygel, CEPETRO/UNICAMP and UiO

Abstract

The imaging of diffracted waves can provide information related to finer geological structures, such as faults and pinch-outs, which reflected waves are not able to provide. Since these waves are weaker than reflections, an approach that enhances and separates diffractions is necessary. In this work, we propose a method to separate diffractions in zero-offset sections using a modified version of the Common Reflection Surface (CRS) method. The CRS operator admits a particular case where the diffractions are stacked coherently, which often leads to a partial separation of events. In order to improve the separation quality, we propose a perturbation factor to be applied to one of the CRS attributes. The application of the proposed method on a 2D real dataset showed good results with a clear separation of events.

Introduction

The conventional seismic processing aim to enhance reflected waves, but the information contained in these waves is not suitable for imaging small geological features such as faults and pinch-outs. However, a significant part of this information is carried by diffracted waves and since these waves are weaker then the reflected, an approach that separates and emphasizes diffractions is necessary.

In order to use this information, several techniques have been developed. Fomel (2002) applied a plane-wave destruction filter to separate diffractions on stacked sections. Landa et al. (1987) proposed a traveltime equation based on the double-square-root operator, specifically to enhance diffractions. Berkovitch et al. (2009) introduced a method based on diffraction stacking events using multifocus. Dell and Gajewski (2011) applied a diffraction-filter based on Common Reflection Surface (CRS) attributes.

In this work, we propose a method to separate diffractions in zero-offset sections using the CRS method, which admits a well known particular case where the diffractions are stacked coherently. Nevertheless, this particular case often leads to a partial separation of events. To counter this limitation and improve this separation we introduce a perturbation factor to one of the CRS attributes, which can be related to the NMO velocity and the curvature of an hypothetical wavefront.

CRS method

The CRS method (e.g. Jäger et al., 2001) can provide a simulated zero-offset section with high signal-to-noise ratio and also extract more attributes of the geological structures. This is possible because the CRS method interprets the subsurface reflectors as an ensemble of reflecting elements, defined not only by points, but also by dip and curvature. By doing so, the CRS stacking operator uses information of source-receiver pairs in the vicinity of the so-called central or reference CMP position, in which the zero-offset trace will be constructed.

The CRS traveltime, Equation 1, can be obtained from a second-order Taylor expansion of the squared traveltime for a given reflector, where t_0 is the normal ray time, h is the half-offset, see Figure 1.

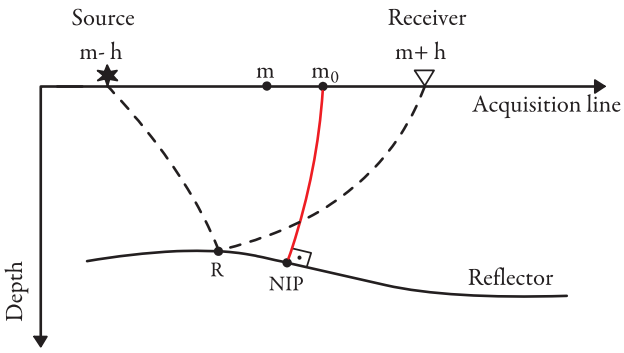

Figure 1: Acquisition geometry with a source in $m-h$, receiver in $m+h$ and midpoint in m with dashed lines representing the paraxial rays. The central or reference CMP in m_0 with the red line representing the normal ray.

$$t^2(m,h) = [t_0 + A\,(m-m_0)]^2 + B\,(m-m_0)^2 + C\,h^2 \qquad (1)$$

The coefficients A, B and C admit physical interpretations (Hubral, 1983) relating to two hypothetical wavefronts emerging on the acquisition surface at the m_0 position, described by the following equations:

$$A = \frac{2\,sen\beta}{v_0}, \quad B = \frac{2\,t_0\,cos^2\beta}{v_0}K_N \quad \text{and} \quad C = \frac{2\,t_0\,cos^2\beta}{v_0}K_{NIP}. \qquad (2)$$

These coefficients carry information about geologic attributes, namely: β, K_{NIP} and K_N. The parameter A can be understood as the slowness of the normal ray emerging at m_0, which is related to its emergence angle β and the near-surface velocity, v_0. The parameter C is related to the curvature K_{NIP} of a hypothetical wavefront, called NIP wave, emerging at m_0 from a point source at the incidence point of the normal ray or NIP (Normal Incidence Point), as seen in Figure 2 (a). The parameter B is related

to the curvature, K_N, of another hypothetical wavefront, called Normal wave, that originates in a region around the normal incidence point as an exploding reflector, as seen in Figure 2 (b).

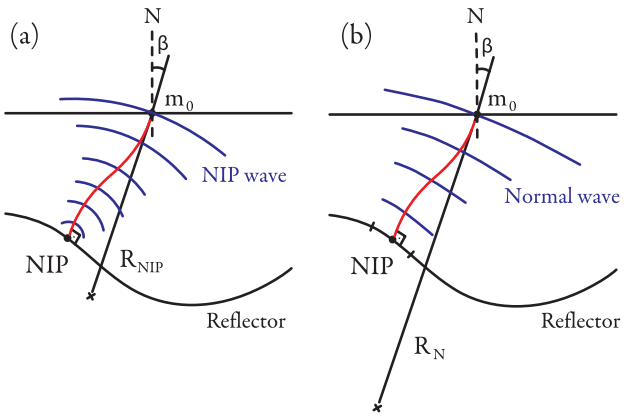

Figure 2: (a) NIP-wave and its curvature radius, R_{NIP}. (b) Normal wave and its curvature radius, R_N. Both described for a non-homogeneous medium with the normal ray in red.

In order to estimate the CRS parameters we are using a strategy that divides the pre-stack dataset in two subdomains (Figure 3) and perform estimations for all CMPs and time samples. The first subdomain is a CMP gather, where $m = m_0$ in Equation 1. In this case, the traveltime Equation 3 depends only on the parameter C and it is estimated using semblance (Neidel and Taner, 1971).

$$t^2(m_0,h) = t_0^2 + C\,h^2 \tag{3}$$

This estimation is very similar to a conventional velocity analysis, where the term Ch^2 can be understood as the $(4h^2)/v_{NMO}^2$ term in the CMP method. Thus, the parameter C also carries information about the velocity model. The second subdomain is a zero-offset section, where $h = 0$ in Equation 1. Now, the traveltime Equation 4 depends on two parameters, A and B. With the zero-offset section obtained stacking the dataset with the estimated C, the parameter A can be estimated by linear estimation, assuming $B = 0$ for small apertures.

$$t^2(m,0) = [t_0 + A\,(m-m_0)]^2 + B\,(m-m_0)^2 \tag{4}$$

Finally, the parameter B can be estimated using larger apertures, taking into account the parameter A found in the previous estimation. In both cases, they are also estimated by semblance.

CRS method for diffractions

Although the CRS stacking aims to enhance reflection events, this technique can also be adapted to enhance diffractions. This is possible considering a diffractor as a limiting case when a reflector shrinks to a point, which leads to $K_N = K_{NIP}$ for diffractions. Applying this condition in Equation 2 and then in Equation 1, we have

$$t^2(m,h) = [t_0 + A\,(m-m_0)]^2 + C\,[(m-m_0)^2 + h^2]. \tag{5}$$

With these assumptions, Equation 5 presents a better fit for a possible diffraction event that passes through a certain point in the zero-offset section, favoring the diffractions rather than reflections on the coherence analysis. Observe that Equation 5 depends only on two parameters, A and C, unlike Equation 1 which depends on three.

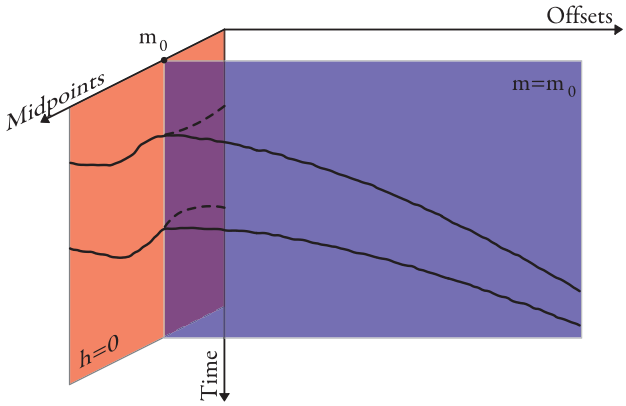

Figure 3: Dataset with estimation sudomains highlighted: CMP domain, case when $m = m_0$, in blue; ZO domain, case when $h = 0$, in orange.

Now, applying the same estimation strategy described above to the case of diffractions (Equation 5) we obtain once again the Equation 3 to estimate the parameter C and

$$t^2(m,0) = [t_0 + A\,(m-m_0)]^2 + C\,(m-m_0)^2, \tag{6}$$

to estimate the parameter A. Note that, in the case of the CMP subdomain, the estimate of parameter C does not change in relation to the conventional CRS method. Thus, the estimate of A could be performed along the curve described by Equation 6 because the values of C are known for all points of the stacked section.

Perturbation factor ε

In order to improve the separation of reflection and diffraction events, we will introduce a perturbation factor ε multiplying parameter C in Equation 6, which results in

$$t^2(m,0) = [t_0 + A\,(m-m_0)]^2 + \varepsilon\,C\,(m-m_0)^2. \tag{7}$$

The perturbation factor ε varies in the neighborhood of 1 and aims to counteract errors in the initial estimate of parameter C, which may compromise the outcome of the estimation of parameter A. Moreover, the apparent velocity along the diffraction can vary because of its displacement in relation to the reference CMP position, m_0. So, the application of a perturbation factor on parameter C can also be seen as a perturbation in the medium velocity, since it changes the asymptotes of the diffraction hyperbola defined by Equation 7. This process is illustrated in Figure 4.

With these modifications, a simultaneous estimation of A and ε can be performed over larger apertures with the advantage that the reflection events are further attenuated because a better choice of apertures to implement the condition $B \approx C$.

Finally, the CRS stack for diffractions can be performed using this perturbed operator

$$t^2(m,h) = [t_0 + A\,(m-m_0)]^2 + C\,[\varepsilon\,(m-m_0)^2 + h^2], \tag{8}$$

which stacks diffractions more efficiently than simply assuming $B = C$ on the conventional CRS operator.

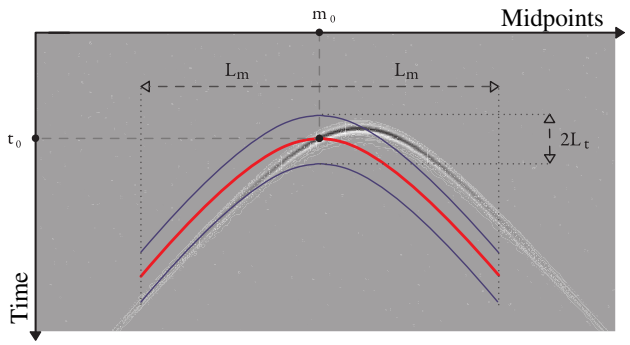

(a) Diffraction traveltime for $\beta = 0$ and $\varepsilon = 1$ at point (m_0, t_0).

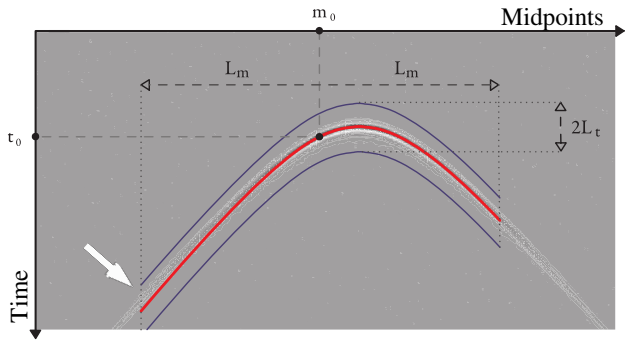

(b) Diffraction traveltime for $\beta = -37$ and $\varepsilon = 1$ at point (m_0, t_0). The white arrow indicates an small adjustment error over the diffractions sides.

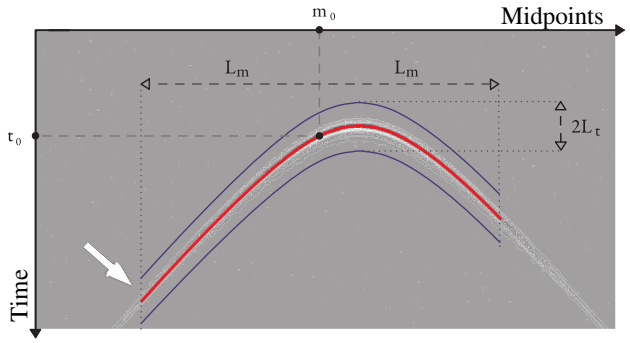

(c) Diffraction traveltime for $\beta = -37$ and $\varepsilon = 0.95$ at point (m_0, t_0). Now, the white arrow shows an better fit to the diffraction event.

Figure 4: Diffraction traveltime (Equation 7) plotted in red for different values of β and ε for a given point (m_0, t_0) along a diffraction event. The estimation is performed with an aperture of $2L_m$ in midpoints and $2L_t$ in time.

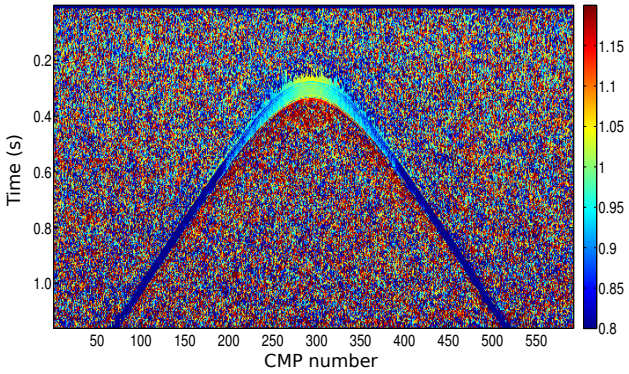

Figure 5: Perturbation factor ε estimated for each point (m_0, t_0) along a diffraction event.

Data examples

The proposed method was applied to a 2D marine dataset acquired in 1985 over the Jequitinhonha Basin, Brazil. The dataset has the following acquisition parameters: 1577 shots with intervals of 25 m, 120 hydrophones in intervals of 25 m and a time sampling of 4 ms.

Following the steps described above, the estimation of parameter C was performed with an aperture of $500\ m$. The dataset was stacked with the obtained velocity model, as shown in Figure 6, where it is possible to note the presence of diffractions, especially along the seafloor. This stacked section was used to estimate simultaneously the parameter A and the perturbation factor ε with estimation intervals of $\pm 65^\circ$ and 0.8 to 1.2, respectively. Figures 7 and 8 show these results. In this case, the aperture size was chosen in order to be comparable to the size of the difractions observed on the initial stacked section (about $800\ m$). The semblance panel obtained for this estimation can be seen in Figure 9, where is possible to observe a visible separation of events. Figure 10 shows the CRS stack for diffractions obtained with the proposed approach.

Conclusions

The CRS operator admits a well known particular case where it can stack diffractions coherently rather than reflections. However, the results obtained using this approach often lead to a partial separation of events. In order to improve this separation we propose a method to enhance only diffractions using perturbed CRS attributes, which maintain the same complexity than the conventional CRS in terms of number of parameters to estimate.

The proposed method was implemented and applied on a 2D marine dataset. The obtained CRS stack for diffractions demonstrated an evident separation of events even with strong reflections obscuring or crossing these events.

References

Berkovitch, A., I. Belfer,Y. Hassin and E. Landa, 2009, Diffraction imaging by multifocusing: Geophysics, **74**, WCA75-WCA81.

Dell, S. and D. Gajewski, 2011, Common-reflection-surface-based workflow for diffraction imaging. Geophysics, v. **76**, n. 5, p.S187-S195.

Fomel, S., 2002, Applications of plane-wave destruction filters: Geophysics, **67**, 1946-1960.

Hubral, P., 1983, Computing true amplitude reflections in a laterally inhomogeneous earth: Geophysics, **48**, 1051-1062.

Jäger, R., J. Mann, G. Höcht and P. Hubral, 2001, Common-reflection-surface stack: image and attributes. Geophysics, **66**, 97-109

Landa, E., V. Shtivelman and B. Gelchinsky, 1987, A method for detection of diffracted waves on common-offset sections: Geophysical Prospecting, **35**, 359-373.

Neidel, N. S., and M. Taner, 1971, Semblance and other coherency measures for multichannel data: Geophysics, **36**, 482-497.

Acknowledgments

We acknowledge the support of PETROBRAS - SCTC/CEPETRO and the Brazilian agencies: Research Foundation of the State of São Paulo (FAPESP) and the National Council of Scientific and Technological Development (CNPq).

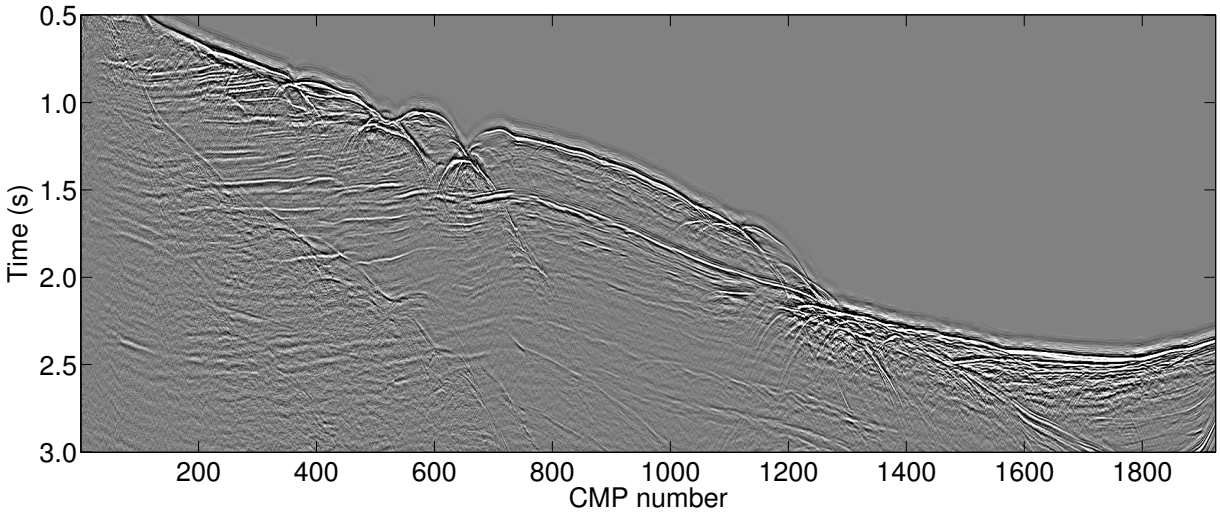

Figure 6: CMP stacked section, obtained after the estimation of parameter C. This section will be used to estimate parameter A and the perturbation factor ε.

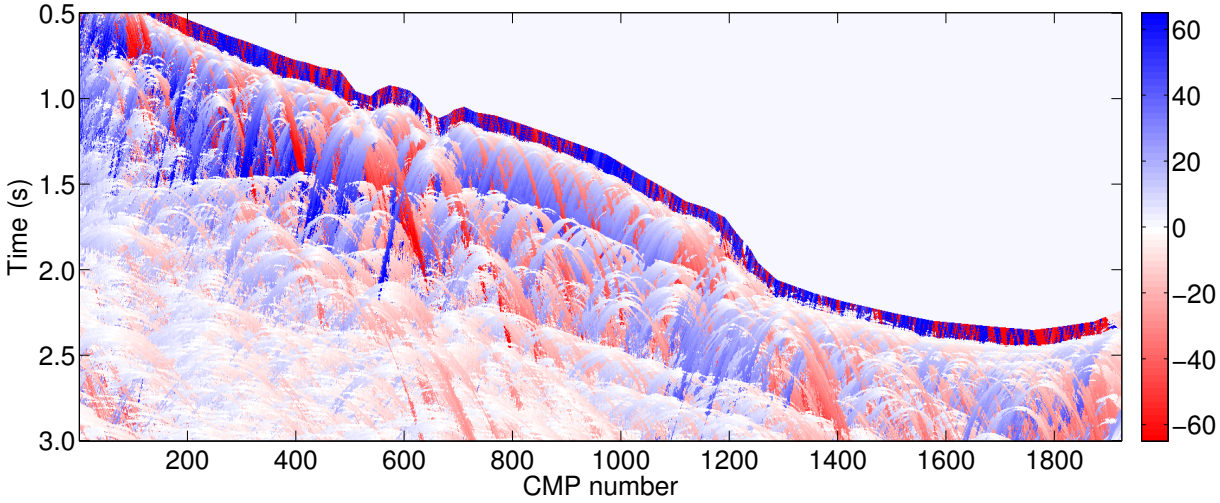

Figure 7: Obtained results for parameter A (converted in emergence angles, β) using the estimation interval of $-65°$ to $65°$.

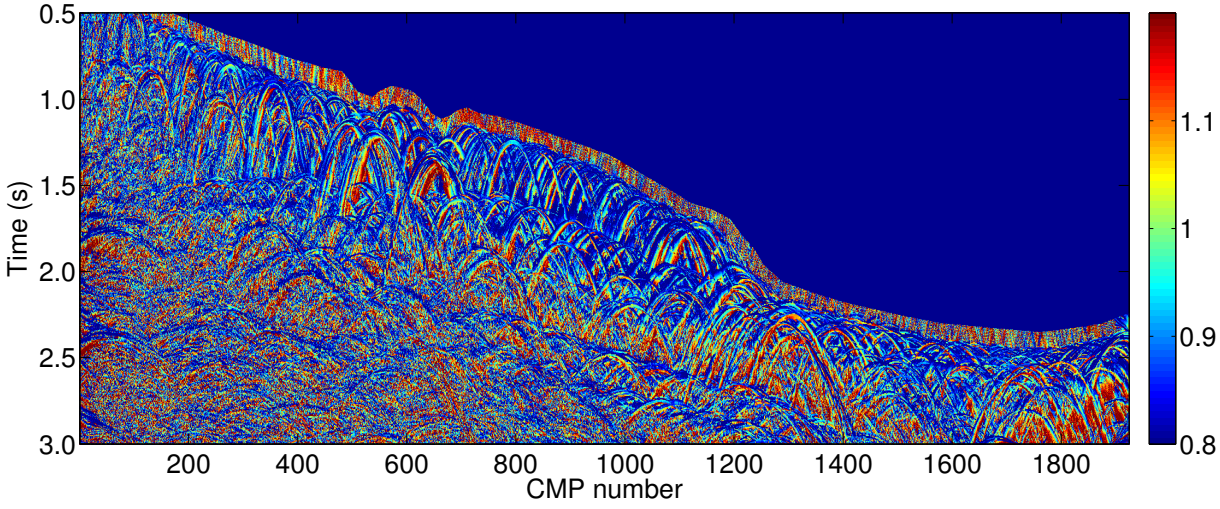

Figure 8: Obtained results for perturbation factor ε using the estimation interval of 0.8 to 1.2.

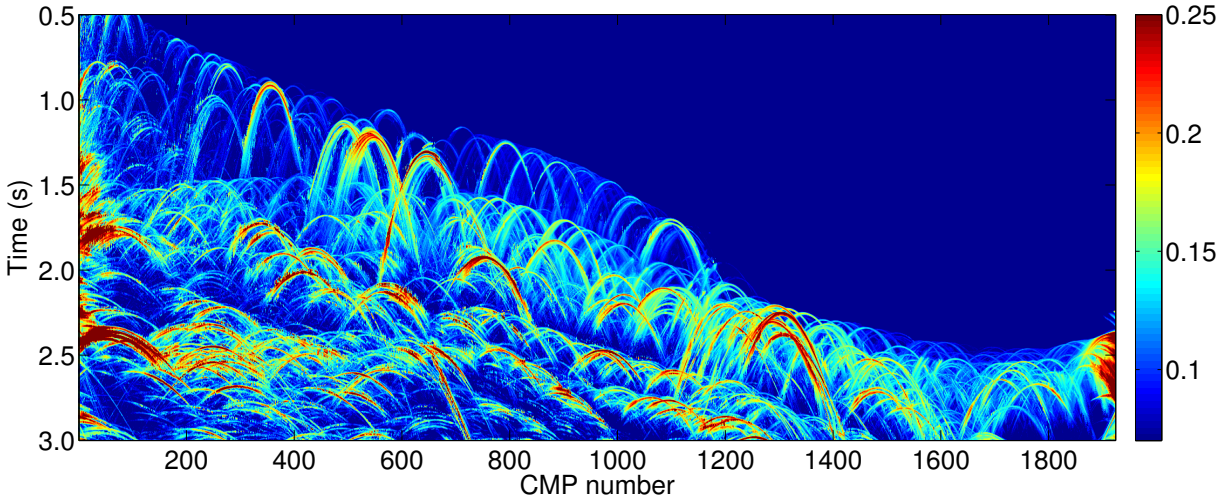

Figure 9: Semblance panel obtained estimating simultaneously the parameter A and the perturbation factor ε.

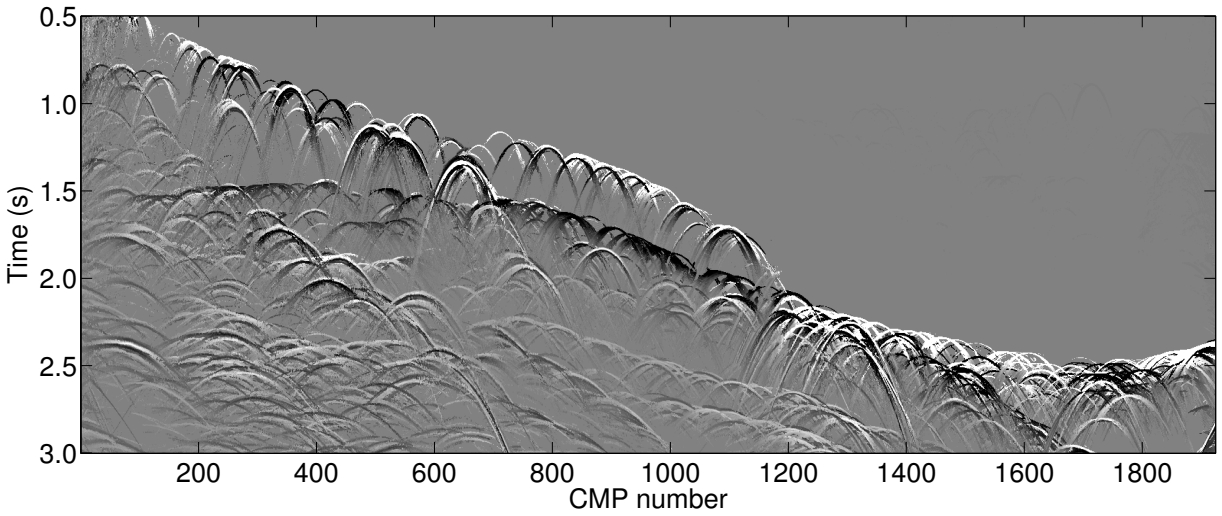

Figure 10: CRS stack for diffractions using parameters A, C and ε.